Effects of cavitation in a nozzle on liquid jet atomization

Sou, Akira
Hosokawa, Shigeo
Tomiyama, Akio

(Citation)
International Journal of Heat and Mass Transfer,50(17-18):3575-3582

(Issue Date)
2007-08

(Resource Type)
journal article

(Version)
Accepted Manuscript

(URL)
https://hdl.handle.net/20.500.14094/90000581

International Journal of Heat and Mass Transfer, Vol. 50, Iss. 17-18, (2007) pp. 3575-3582
http://dx.doi.org/10.1016/j.ijheatmasstransfer.2006.12.033

Effects of Cavitation in a Nozzle on Liquid Jet Atomization

Akira Sou *, Shigeo Hosokawa, Akio Tomiyama

Faculty of Engineering, Kobe University, 1-1 Rokkodai, Nada, Kobe 657-8501, Japan

* Corresponding author, sou@mech.kobe-u.ac.jp (Akira Sou).

Received 24 April 2006; received in revised from 6 November 2006;
Available online 26 March 2007

Abstract

Cavitation in two-dimensional (2D) nozzles and liquid jet in the vicinity of the nozzle exit were visualized using high-speed cameras to investigate the effects of cavitation on liquid jet under various conditions of cavitation and Reynolds numbers σ and *Re*. Liquid velocity in the nozzle was measured using a laser Doppler velocimetry to examine the effects of cavitation on the flow in the nozzle and liquid jet. As a result, the following conclusions were obtained: (1) cavitation in the nozzles and liquid jet can be classified into the four regimes: (no cavitation, wavy jet), (developing cavitation, wavy jet), (super cavitation, spray) and (hydraulic flip, flipping jet), (2) liquid jet near the nozzle exit depends on cavitation regime, (3) cavitation and liquid jet are not strongly affected by *Re* but by σ, and (4) strong turbulence induced by the collapse of cavitation clouds near the exit plays an important role in ligament formation.

Keywords: Cavitation; Liquid jet; Atomization; Visualization; Ligament; Internal flow

Nomenclature

L_{cav}	streamwise length of cavitation zone
L_{cav}*	normalized cavitation length (=L_{cav} / L_N)
L_N	nozzle length [mm]
P_a	atmospheric pressure [Pa]
P_v	vapor saturation pressure [Pa]
Re	Reynolds number
t	time [μs]
t_N	nozzle thickness [mm]
T_L	liquid temperature [K]
V_N	mean liquid velocity in a nozzle [m/s]
W_N	nozzle width [mm]
x	horizontal distance from nozzle center [mm]
y	vertical distance from nozzle inlet [mm]

Greek symbols

γ	surface tension [N/m]
ν_L	liquid kinematic viscosity [m^2/s]
θ	spray angle [deg.]
ρ_L	liquid density [kg/m^3]
σ	the cavitation number

Subscripts

N	nozzle
L	liquid

1. Introduction

It has been pointed out through a number of experimental studies [1-5] that cavitation takes place in the nozzle of pressure atomizers, such as fuel injectors for diesel engines and rocket engines, and affects the characteristics of a discharged liquid jet. Hiroyasu et al. [1] showed that liquid jet atomization was promoted when cavitation extended from the inlet to the exit of a nozzle. Since the shapes of the nozzles used in most of the previous studies have been cylindrical [1-5], it has been difficult to measure liquid velocity, turbulence intensity and radial distribution of cavitation bubbles in nozzles. Hence, several studies have been carried out using two-dimensional (2D) nozzles for visualization of detailed cavitation behavior [6-8]. However systematic

observations of cavitation including incipient cavitation and well-developed cavitation have not been carried out yet. Recently some attempts have been made to measure the velocity in the nozzle which might play an important role in liquid jet atomization [9-12]. However the liquid velocity and its fluctuation under well-developed cavitation condition have not been measured yet. Hence, the mechanism of atomization enhancement by cavitation has not been clarified yet.

In the present study, cavitation in 2D nozzles and liquid jet in the vicinity of the nozzle exit were visualized using a digital camera and high-speed video cameras under various conditions of Reynolds and cavitation numbers to examine the effects of the two dimensionless numbers on cavitation and liquid jet and to investigate the atomization enhancement mechanism by cavitation. Liquid velocity in the 2D nozzle was measured by using a laser Doppler velocimetry (LDV) to investigate the effects of cavitation on the flow in the nozzle and liquid jet atomization.

2. Experimental Setup

2.1. Liquid injection system

Schematic of experimental setup is shown in Fig. 1. Filtered tap water or light oil was discharged from 2D nozzles into ambient air by the plunger pump through the cylindrical air separation tank of 90 mm in inner diameter and 800 mm in height. Liquid flow rate was measured using a flowmeter (Nippon flow cell, D10A3225) in the upstream of the nozzle. As shown in Fig. 2, the 2D nozzle consists of two acrylic flat plates and two stainless steel thin flat plates, by which sharp-edges were formed at the inlet of the nozzle. To examine the effect of nozzle size on the cavitation and liquid jet characteristics, two nozzles of different sizes were used. The width W_N, length L_N and thickness t_N of a nozzle were 4, 16 and 1 mm, and those of the half scale nozzle were 2, 8 and 0.5 mm, respectively (L_N / W_N = 4). This nozzle shape enabled us to measure not only streamwise but also lateral component of the liquid velocity by LDV.

2.2. Imaging and LDV systems

Images of cavitation and liquid jet were taken by using a digital camera (Nikon, D70, 3008 x 2000 pixels) and a flush lamp whose duration was 12 μs. Time evolution of cavitation in the nozzle and liquid jet were visualized using either an ultra high-speed digital video camera (nac, IMACON 200, 1200 x 980 pixels, exposure time t_{EX} = 5 ns, frame rate = 100000 fps) or a high-speed digital video camera (Redlake, Motion Pro HS-1, 32 x 1280 pixels, frame rate = 20000 fps, shutter speed = 50 μs). Streamwise and lateral components of velocity in the larger nozzle were measured using an LDV system (DANTEC, 60X series), whose measurement uncertainty was within 1 %.

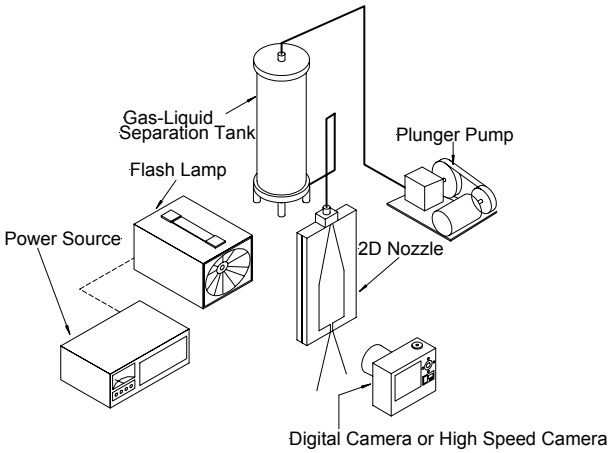

Fig. 1. Experimental setup.

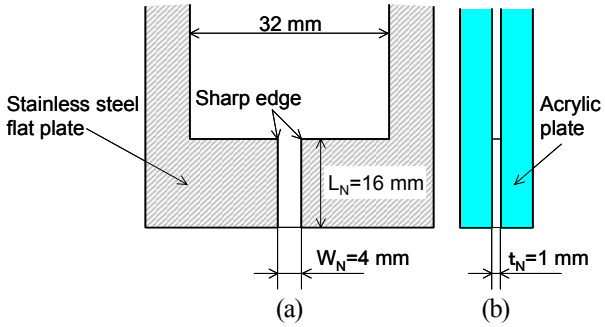

Fig. 2. 2D Nozzle (W_N = 4 mm, L_N = 16 mm, t_N = 1 mm): (a) front view; (b) side view.

2.3. Experimental conditions

Experiments were conducted at various conditions of cavitation number σ and Reynolds number *Re*, which are defined by the following equations:

$$\sigma = \frac{P_a - P_v}{0.5\rho_L V_N^{\,2}} \tag{1}$$

$$Re = \frac{V_N W_N}{\nu_L} \tag{2}$$

where P_a is the atmospheric pressure, P_v the vapor saturation pressure, ρ_L the liquid density, V_N the mean liquid velocity in the nozzle, ν_L the liquid kinematic viscosity. These parameters were controlled by changing the liquid flow rate, fluid properties and nozzle size. Typical experimental conditions are listed in Table 1 (water, T_L = 292 K, W_N = 4 mm). The maximum error

of measured flow rate was 2.7 % for the larger nozzle and 3.7 % for the half scale nozzle. The concentration of dissolved oxygen (*DO*) in water was 9.0 mg/*l*, when the water temperature T_L was 291 K. In more than 100 images of the flow in the nozzle (spatial resolutions were 2 μm/pixel) no micro bubbles or solid particles were observed in the upstream of cavitation zone. The LDV measurement could not be carried out unless silicone carbide (SiC) particles of 3 μm in mean diameter were added as seeding particles (2.5 g/m^3). The effects of the added particles on cavitation were negligible [13].

Table 1 Typical experimental conditions and flow regimes (water, T_L = 292 K, W_N = 4 mm)

Reynolds number, *Re*	Cavitation number, σ	Cavitation in nozzle	Liquid jet
45000	1.57	No cavitation	Wavy jet
50000	1.27		
58000	0.94	Developing cavitation	
64000	0.78		
68000	0.69	Super cavitation	Spray
70000	0.65		
76000	0.55	Hydraulic flip	Flipping jet
78000	0.52		

3. Results and Discussion

3.1. Flow regimes

Flow regimes in the nozzle and liquid jet near the nozzle exit are summarized in Fig. 3 and Table 1 (water, T_L = 292 K, W_N = 4 mm). When σ > 1.2, cavitation bubbles were not observed and liquid jet took the form of "wavy jet". For 0.75 ≤ σ ≤ 1.2, cavitation bubble clouds appeared in the upper half of the nozzle. We defined this type of the cavitation as "developing cavitation". In developing cavitation, liquid jet near the exit was wavy jet. For 0.55 < σ < 0.75, cavitation zone extended from the inlet to just above the nozzle exit (normalized mean cavitation length L_{cav}* ≃ 0.8-0.9, where the definition of L_{cav}* will be described later). We named this regime "super cavitation". In super cavitation, liquid jet atomization was enhanced, i.e., ligaments and droplets appeared ("spray") and the spray angle increased. Further decrease in σ (σ < 0.55) resulted in the formation of "hydraulic flip" and "flipping jet", in which liquid flow separated at one inlet edge and did not reattach to the side wall. The condition of the incipient cavitation has been examined in our previous report [13].

Figure 4 shows the distribution of mean liquid velocity in a nozzle of 4 mm in width. We confirmed that cavitation appeared within the separated boundary layer (SBL). The distribution of mean velocity was not uniform just below the cavitation zone, i.e. the reattachment point of SBL, however it became almost uniform near the nozzle exit in no cavitation or developing cavitation regimes.

3.2. Effects of σ and Re on cavitation and liquid jet

The Reynolds number *Re* increases with water temperature T_L since kinematic viscosity ν_L of water decreases with increasing T_L, while the cavitation number σ does not change a lot by varying T_L. To examine the influences of σ and *Re* on cavitation and liquid jet, observations were conducted under various T_L conditions (293 ≤ T_L ≤ 333 K). Regimes of cavitation and liquid jet are shown in Figs. 5(a) and (b), respectively. The spray region on the liquid jet regime map corresponds to the

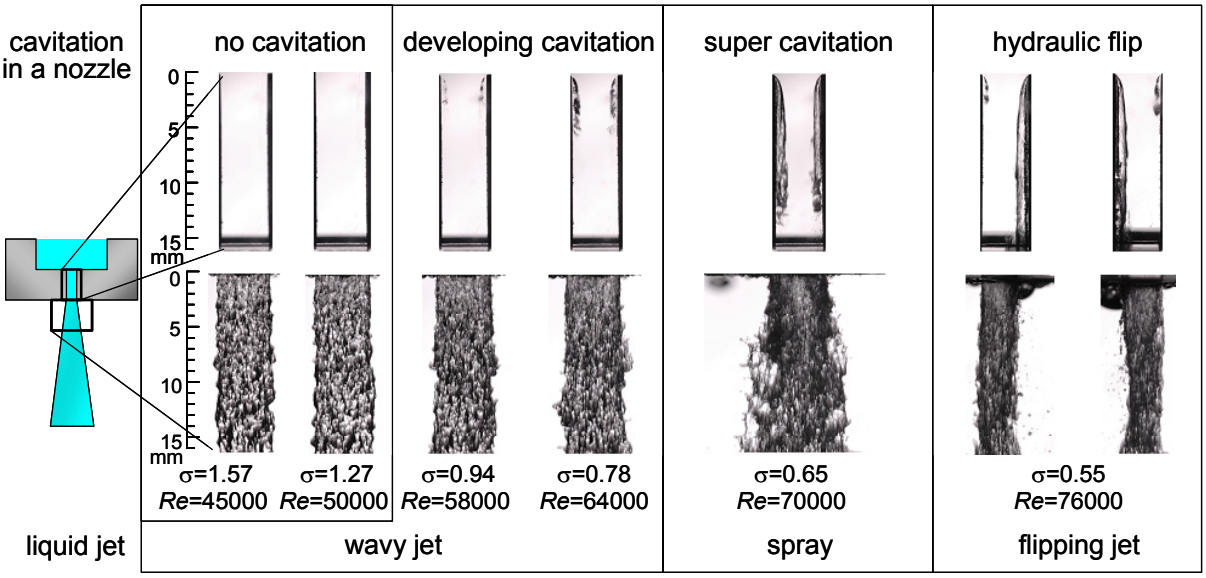

Fig. 3. Images of cavitation in a 2D nozzle and liquid jet (water, T_L = 292 K, W_N = 4 mm, flush duration = 12 μs).

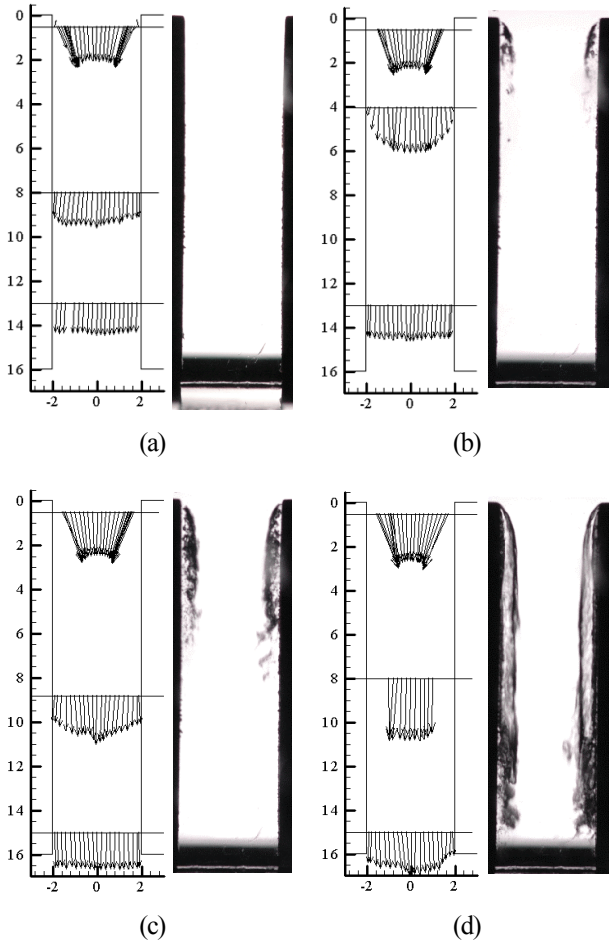

Fig. 4. Distributions of mean liquid velocity in a 2D nozzle (water, T_L = 291 K, W_N = 4 mm): (a) σ =1.27, Re=50000, (b) σ =0.95, Re=58000, (c) σ =0.78, Re=64000, (d) σ =0.65, Re=70000.

super cavitation region on the cavitation regime map, which means that the formation of super cavitation enhances liquid jet atomization. Since the transition from developing to super cavitation does not strongly depend on *Re* but on σ, the transition from wavy jet to spray also depend on σ.

The normalized cavitation lengths (=streamwise length of cavitation zone L_{cav} / nozzle length L_N) were measured from the nozzle images in the cases of the larger nozzle, the half scale nozzle (T_L = 293 K) and light oil (W_N = 4 mm). The effects of *Re* and σ on the averaged value L_{cav}* of the normalized cavitation lengths are shown in Figs. 6(a) and (b), respectively. The maximum fluctuation of the normalized cavitation length was 0.05 for developing cavitation and 0.15 for super cavitation. Regime transition in the cases of the half scale nozzle and light oil showed the same trends as that in the larger nozzle. The L_{cav}* did not strongly depend on *Re* but on σ.

Spray angles in the vicinity of the nozzle exit (15 mm downstream of the nozzle exit) were measured from the images as shown in Fig. 7, and the averaged values θ are plotted against L_{cav}* in Fig. 8. The maximum fluctuation of measured spray angle was 1.8 degree for developing cavitation and 5.4 degree for super cavitation. When the value of L_{cav}* is about 0.8-0.9, i.e. in super cavitation, θ increases as shown in Fig. 8. The difference in spray angle between water (surface tension γ = 0.073 N/m), the half scale nozzle and light oil (γ = 0.03 N/m) for L_{cav}* smaller than about 0.8 was due to the difference in surface tension.

The lateral component of mean velocity *U* and the RMS of lateral component of velocity fluctuation *u'* (turbulence intensity) near the exit (distance from the inlet *y* = 15 mm) are shown in Fig. 9 to examine the effects of cavitation on turbulence intensity and liquid jet. In developing cavitation (σ = 0.78) the value of *U* near the exit was close to zero and *u'* was small. On the other hand, *u'* in super cavitation (σ = 0.65) was large and the value of *U* was positive, i.e., the mean flow directed toward the side wall. The lateral flow and strong turbulence in super cavitation could be the dominant mechanisms to increase the spray angle and initiate atomization.

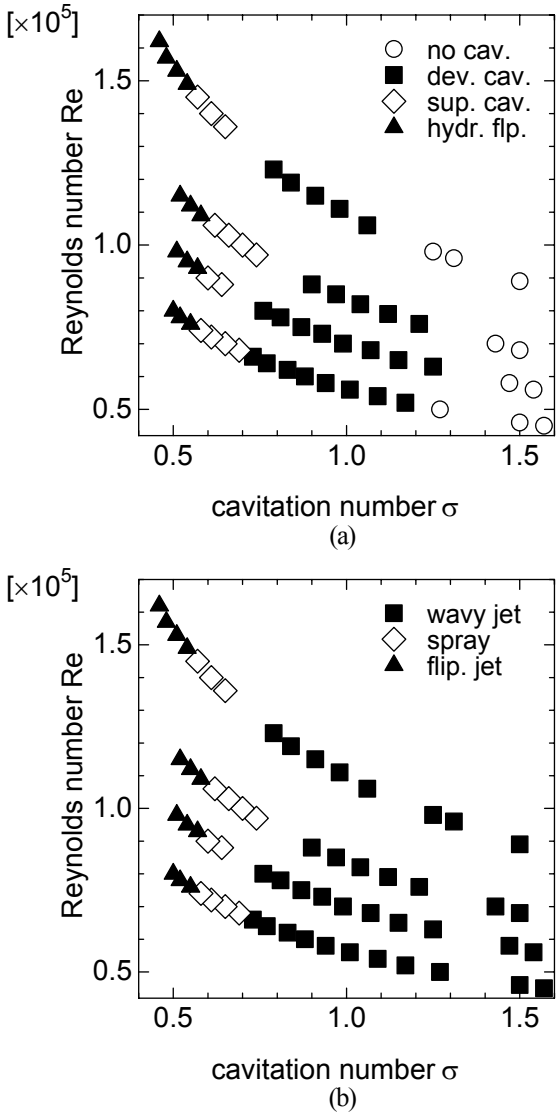

Fig. 5. Effects of σ and *Re* on cavitation and liquid jet (water, W_N = 4 mm, T_L = 293, 303, 313, 333 K): (a) cavitation regime map; (b) liquid jet regime map.

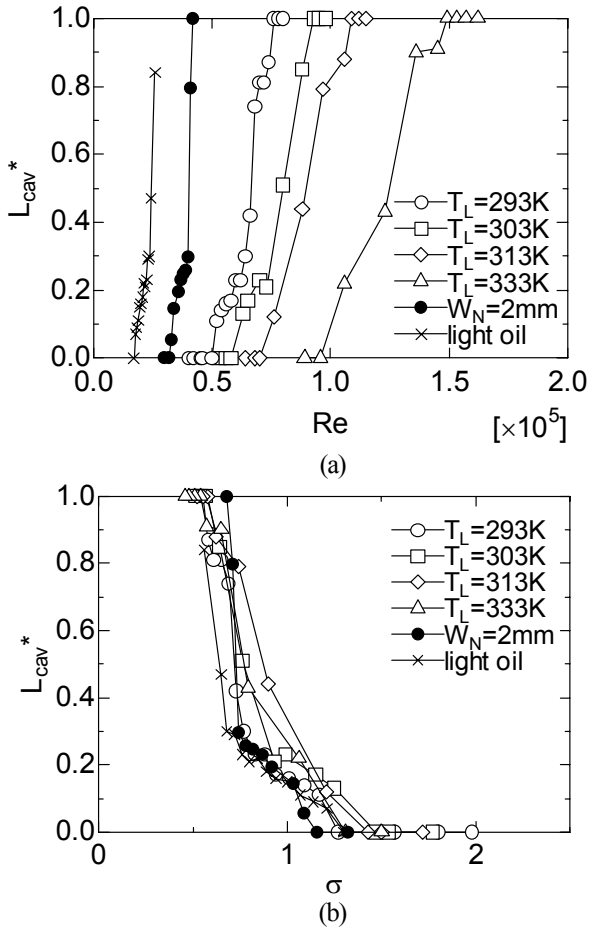

Fig. 6. Effects of *Re* and σ on normalized cavitation length L_{cav}*: (a) effects of *Re* on L_{cav}*; (b) effects of σ on L_{cav}*.

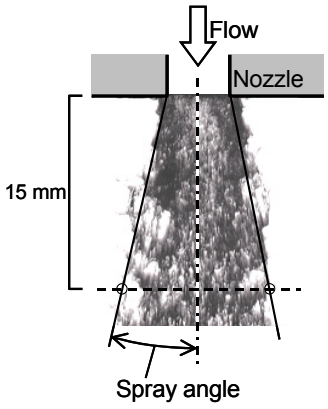

Fig. 7. Spray angle θ.

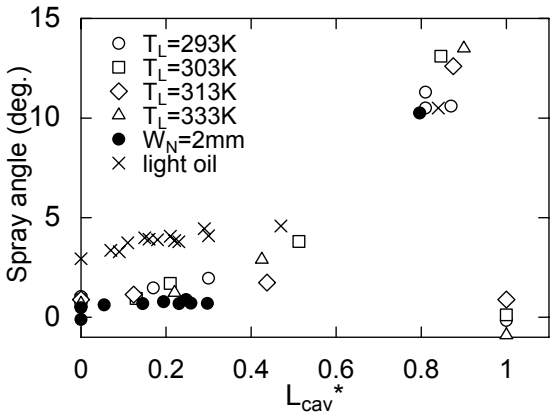

Fig. 8. Effects of L_{cav}* on spray angle θ.

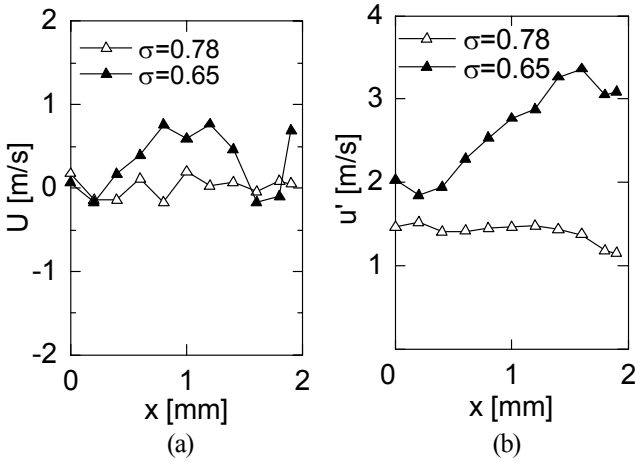

Fig. 9. Lateral component of velocity above the nozzle exit (water, T_L = 291 K, W_N = 4 mm, y = 15 mm): (a) mean velocity, (b) turbulence intensity.

3.3. Effects of cavitation collapse on ligament formation

Cavitation behavior near the nozzle exit in super cavitation was visualized using the ultra-high speed camera (t_{EX} = 5 ns, 100000 fps). Images of the collapse of cavitation cloud are shown in Fig. 10 (water, T_L = 292 K, W_N = 4 mm, σ = 0.69). The collapse of cavitation clouds took place intermittently. The collapse might cause a high turbulence intensity near the exit, and therefore affects the ligament formation.

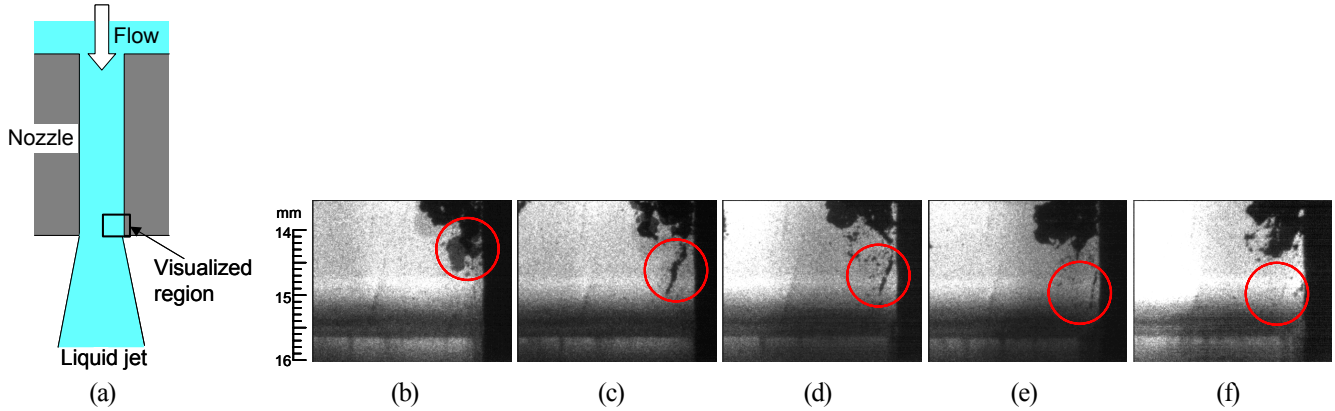

Fig. 10. Collapse of cavitation clouds above the nozzle exit (water, T_L = 292 K, W_N = 4 mm, σ = 0.69, *Re* = 68000, 2.5 μm/pixel, t_{EX} = 5 ns); (a) visualized region, (b) t = 0 μs, (c) t = 30 μs, (d) t = 60 μs, (e) t = 90 μs, (f) t = 120 μs.

To examine the relation between the collapse of cavitation cloud and ligament formation in super cavitation, cavitation and liquid jet interface were visualized simultaneously with a high frame rate (20000 fps). Since the refractive index of the acrylic plate of the nozzle is higher than that of air, an acrylic plate was placed between the liquid jet and the camera to match the optical distances. In the high frame rate imaging, the image size was limited to 32 x 1280 pixels. Hence, the acrylic plate was tilted to capture both cavitation and jet interface within a narrow region shown in Fig. 11.

Time series images of cavitation and liquid jet are shown in Fig. 12 (water, W_N = 4 mm, T_L = 293 K, σ=0.65, 32 x 1280 pixels, 20000 fps). If a high pressure caused by the cavitation collapse is the dominant mechanism of the ligament formation, a ligament may appear immediately after the collapse. However a ligament did not always appear when a collapse took place, and some ligaments appeared when there were no cavitation collapses as shown in Fig. 12. The arrows in the figure represent the paths moving with mean liquid velocity in the nozzle V_N. A ligament was formed, when a trace of cavitation collapse came out with the velocity V_N from the nozzle. By investigating 10000 images it was found that the frequencies of the shedding and collapse of cavitation clouds were about 1-4 kHz in the case of W_N = 4 mm. Figure 13 shows the power spectrum of the mean CCD intensities in the region (32 x 40 pixels) where cavitation clouds pass through (y = 12 mm). A large intensity can be seen in the range of about 1-4 kHz.

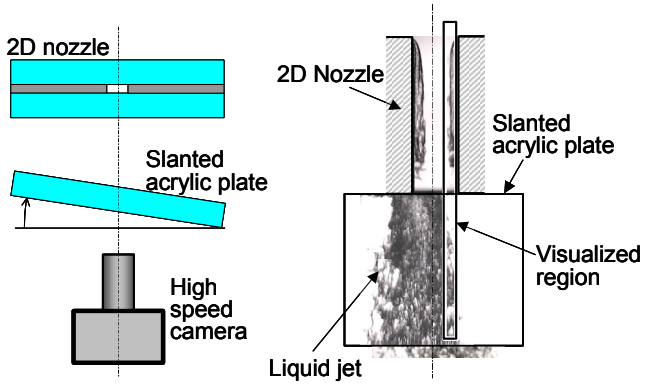

Fig. 11. Experimental setup for the simultaneous visualization of cavitation and liquid jet: (a) top view; (b) front view.

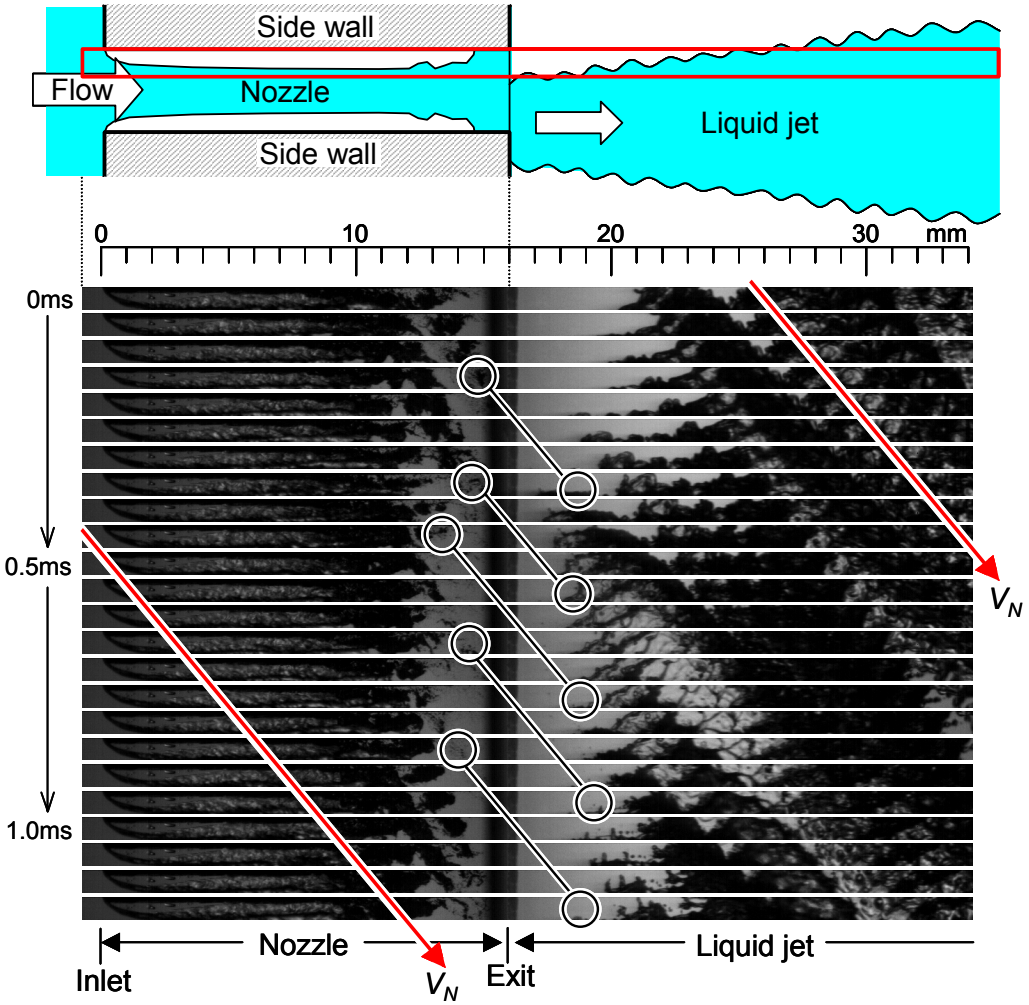

Fig. 12. Simultaneous visualization of cavitation and liquid jet interface (water, T_L = 293 K, W_N = 4 mm, σ = 0.65, 32 x 1280 pixels, 20000 fps).

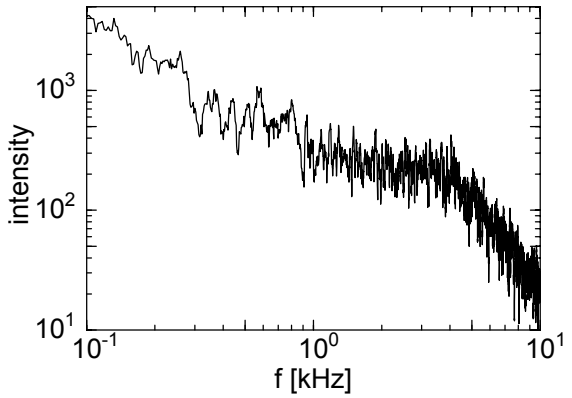

Fig. 13. Power spectrum of image data ($\sigma = 0.65$, super cavitation).

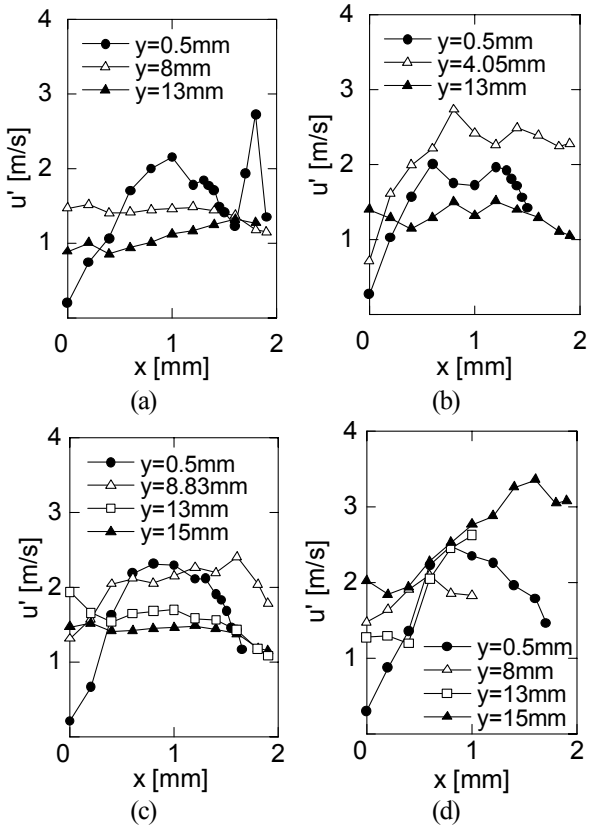

Fig. 14. RMS of lateral component of velocity fluctuation: (a) σ = 1.27, no cavitation; (b) $\sigma = 0.95$, developing cavitation; (c) $\sigma = 0.78$, developing cavitation; (d) $\sigma = 0.65$, super cavitation.

The RMS of lateral component of velocity fluctuation *u'* is plotted in Fig 14. As shown in the figure, strong turbulence appeared just below the cavitation collapse point ($y = 4.05$ mm for $\sigma = 0.95$, $y = 8.83$ mm for $\sigma = 0.78$, $y = 15$ mm for $\sigma = 0.65$), and the turbulence decreased as y increased. This indicates that turbulence intensity increases just below the collapse point, and the strong turbulence reaches the nozzle exit only in the case of super cavitation. The power spectrum of the lateral component of the measured velocity near the exit ($y = 15$ mm) is shown in Fig. 15. A large intensity appeared in the range of about 1-4 kHz for super cavitation ($\sigma = 0.65$). The frequency range agreed with that of the cavitation shedding and the ligament formation. Hence, we could confirm that the strong turbulence induced by the collapse of cavitation clouds near the exit plays an important role in ligament formation.

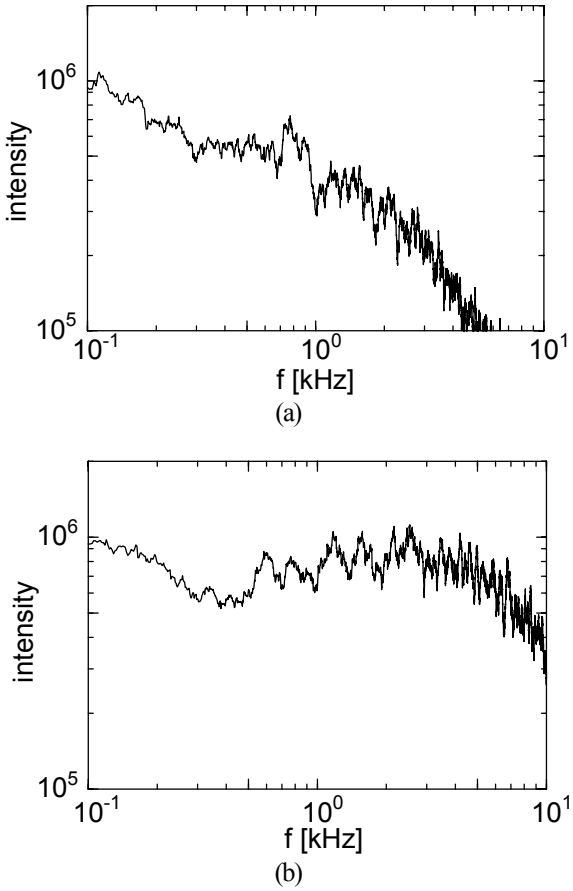

Fig. 15. Power spectrum of LDV data near the exit ($y = 15$mm): (a) σ=0.78, developing cavitation; (b) σ=0.65, super cavitation.

4. Conclusions

Cavitation in two-dimensional (2D) transparent nozzles and liquid jets in the vicinity of the nozzle exit were visualized using a digital camera, an ultra high-speed video camera and a high-speed video camera. Liquid velocity in the 2D nozzle was measured using a LDV system. The effects of the cavitation number σ and the Reynolds number *Re* on cavitation in the nozzle and liquid jet were examined by varying the liquid flow rate, fluid properties and nozzle size. Cavitation in the nozzle and ligament formation at liquid jet interface were simultaneously visualized using a high-speed camera to examine the mechanism of atomization enhancement by cavitation. As a result, the following conclusions were obtained.

(1) Cavitation in 2D nozzles and liquid jet are

classified into the following regimes: 1 – no cavitation, wavy jet; 2 – developing cavitation, wavy jet; 3 – super cavitation, spray; and 4 – hydraulic flip, flipping jet.

(2) Liquid jet atomization near the nozzle exit depends on cavitation regime, i.e., ligament formation and spray angle depend on the normalized cavitation length L_{cav}*.

(3) Cavitation and a liquid jet near the nozzle exit are not strongly affected by the Reynolds number *Re* but by the cavitation number σ.

(4) Strong turbulence induced by the collapse of cavitation clouds near the exit plays an important role in ligament formation.

Acknowledgements

The authors would like to express their thanks to Mr. Shinji Nigorikawa and Mr. Tatsutoshi Maeda. This study was supported by a Grant-in-Aid for Scientific Research (# 16760129) of the Japan Ministry of Education, Culture, Science, Sports and Technology (MEXT) and a Grant-in-Aid for Scientific Research (# 18560170) of the Japan Society for the Promotion Science (JSPS).

References

[1] H. Hiroyasu, M. Arai, M. Shimizu, Break-up Length of a Liquid Jet and Internal Flow in a Nozzle, *Proc. ICLASS - 91* (1991) 275-282.

[2] H. Chaves, M. Knapp, A. Kubitzek, F. Obermeier, T. Schneider, Experimental Study of Cavitation in the Nozzle Hole of Diesel Injectors Using Transparent Nozzles, *SAE Paper*, Paper No. 950290 (1991) 645-657.

[3] C. Soteriou, R. Andrews, M. Smith, Direct Injection Diesel Sprays and the Effect of Cavitation and Hydraulic Flip on Atomization, *SAE Paper*, Paper No. 950080, (1995).

[4] L. C. Ganippa, , G. Bark, S. Andersson, J. Chomiak, Comparison of Cavitation Phenomena in Transparent Scale-up Single-Hole Diesel Nozzles, *Proc. CAV2001* (2001) A9.005.

[5] N. Tamaki, M. Shimizu, H. Hiroyasu, Enhancement of the Atomization of a Liquid Jet by Cavitation in a Nozzle Hole, *Atomization and Sprays*, 11 (2001) 125-137.

[6] M. E. Henry, S. H. Collicott, Visualization of Internal Flow in a Cavitating Slot Orifice, *Atomization and Sprays*, 10 (2000) 545-563.

[7] H. Iida, E. Matsumura, K. Tanaka, J. Senda, H. Fujimoto, R. R. Maly, Effect of Internal Flow in a Simulated Diesel Injection Nozzle on Spray Atomization, *Proc. ICLASS 2000* (2000) CD-ROM.

[8] M. Daikoku, H. Furudate, H. Noda, T. Inamura, Effect of Cavitation in the Two-dimensional Nozzle on Liquid Breakup Process, *Proc. ICLASS 2003* (2003) 17-6, CD-ROM.

[9] J. Walther, J. K. Schaller, R. Wirth, C. Tropea, Investigation of Internal Flow in Transparent Diesel Injection Nozzles using Fluorescent Particle Image Velocimetry (FPIV), *Proc. ICLASS 2000* (2000) CD-ROM.

[10] M. Gnirss, K. Heukelbach, C. Tropea, Influence of Nozzle Flow on the Atomization of Liquid Sheets and Round Jets, *Proc. DFG-Priority Program Atomization and Spray Processes* (2004) Paper No. 1.2.

[11] L. He, F. Ruiz, Effect of Cavitation on Flow and Turbulence in Plain Orifices for Highspeed Atomization, *Atomization and Sprays*, 5-6 (1995) 569-584.

[12] T. Oda, Y. Yasuda, Experimental Investigation on Structure of Cavitating Flow and Velocity Field inside a 2-D Hole Nozzle, *Proc. ICLASS 2003* (2003) 12-5, CD-ROM.

[13] A. Sou, A. Tomiyama, S. Hosokawa, S. Nigorikawa, T. Maeda, Cavitation in a Two-Dimensional Nozzle and Liquid Jet Atomization (LDV Measurement of Liquid Velocity in a Nozzle), *JSME Int. J.*, Ser. B, 49-4, (2006) 1253-1259.